Information Sciences Letters
An International Journal

http://dx.doi.org/10.18576/isl/110611

Effects of Bivariation Viscosity and Magnetic Field on Trapping in a Uniform Tube with Peristalsis

N. T. Eldabe[1], *O. M. Abo-Seida*[2], *A. E. Abd El Naby*[3], *and M. Ibrahim*[3,*]

[1] Department of Mathematics, Faculty of Education, Ain Shams University, Cairo, Egypt
[2] Faculty of Computers and Information, Kafr El-Sheikh University, Egypt
[3] Department of Mathematics, Faculty of Science, Damietta University, New Damietta, Egypt

Received: 2 Apr. 2022, Revised: 2 May 2022, Accepted: 15 Jun. 2022
Published online: 1 Nov. 2022

Abstract: In recent papers, Mehdi Lachiheb has considered fluid viscosity through a peristaltic tube and a channel as a function of the radial and axial components. This author discussed the trapping phenomenon at the centerline of a peristaltic tube and a channel, the pressure rise, and the drag (friction) forces without a magnetic field. Considering the importance of magnetohydrodynamic fluids in bioengineering and medical sciences, we discussed the effects of bivariation viscosity and magnetic field on the trapping phenomenon at the centerline, separated flow on the wall surface of the peristaltic tube, the drag (friction) forces, and the pressure rise. To solve the problem under low Reynolds and long wavelength assumptions, the velocity field and pressure gradient as functions of Hartmann number, amplitude ratio, viscosity parameter, and volume flow rate were obtained using the perturbation approach in terms of Hartmann number $(M < 1)$. The peristaltic pumping and augmented pumping regions were discussed through drag (friction) forces and the pressure rising. In addition, separation flow points on the surface of the wall were determined numerically.

Keywords: Fluid with bivariation viscosity; Magnetohydrodynamics; Newtonian fluid; Peristalsis; Separating flow; Trapping

1. Introduction

Many authors considered that some physiological fluids' viscosity is constant and discussed the characteristics of pumping, the trapping phenomenon at the tube's centerline and a channel with peristalsis, and the reflux phenomenon assuming Reynolds' number is low and the wavelength is long [1–5]. Other researchers considered the viscosity of some physiological fluids as a function of the radial component and they discussed the pressure rise, friction force, peristaltic pumping and augmented pumping assuming that the Reynolds number is zero and the wavelength is long [6–16].

Few authors considered the viscosity of some physiological fluids as a function of axial component [17, 18]. One author considered the viscosity of some physiological fluids as a function of radial and axial components and discussed the trapping phenomenon at the centerline of a tube and a channel with peristalsis, reflux phenomenon, and the pumping characteristics in the absence of a magnetic field [19, 20]. Several authors considered the viscosity of some physiological fluids as a function of the rate of strain of the fluids and discussed the drag (friction) forces, pressure rise, peristaltic pumping, and augmented pumping under zero Reynolds number and long wavelength approximations [21–27].
To the best of our knowledge, no study has discussed the trapping and separated flow phenomena of a fluid with bivariable viscosity variation through a peristaltic tube in the presence of a magnetic field. Thus, the present study is the first to explain these phenomena.

The paper is structured as follows. Section 2 provides the modeling and formulation of the problem in cylindrical coordinates in the non-dimensional form with cancelling wave number and Reynolds number. Section 3 presents the rate of volume flow. Section 4 includes the perturbation solution. Section 5 focuses on separated flow (trapping at the boundary). Section 6 discusses peristaltic pumping, augmented pumping, trapping, and separated flow for various physical parameters of interest. The concluding remarks are summarised in Section 7.

* Corresponding author e-mail: mo.ibrahim2112@gmail.com

2. Problem Formulation

2.1. Geometric model

We addressed the creeping flow of a bivariable viscosity Newtonian fluid via an axisymmetric shape in a tube thickness that is uniform with a sin wave propagating along its wall. The fluid is supposed to be in a transverse magnetic field that is constant. For flows with a magnetic Reynolds number that is small, the induced magnetic field is insignificant. The outside electric field is ignored, and the electric field owing to charge polarization is also neglected. The heat generated by viscous and Joule dissipation is ignored. The gravity effect is also ignored, because gravity in the small intestine is transverse to the flow and does not interact with fluid particles. The problem's geometry is depicted in Fig. 1. A wall's equation can be written as

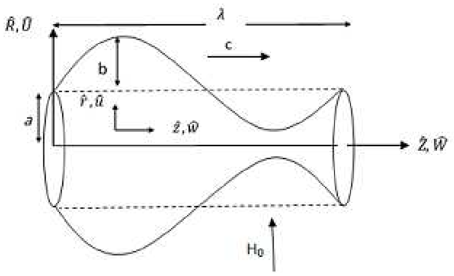

Fig. 1: Sketch of the problem

$$\hat{h} = \hat{a} + \hat{b}\sin\frac{2\pi}{\lambda}(\hat{Z} - c\hat{t}), \tag{1}$$

where $\hat{a}$ is the tube's inlet radius, λ is the wavelength, $\hat{b}$ is the wave's amplitude, $\hat{t}$ is the time and c is the wave speed. The flow in stationary coordinates is unsteady in coordinates that are fixed ($\hat{R}$, $\hat{Z}$), but it can be viewed as steady in the coordinates that are moving ($\hat{r}$, $\hat{z}$), which move at the same speed as the wave in the $\hat{Z}$-direction. The frames have been connected as

$$\hat{Z} = \hat{z} + c\,\hat{t}, \qquad \hat{r} = \hat{R}, \tag{2}$$
$$\hat{W} = \hat{w} + c, \qquad \hat{u} = \hat{U}, \tag{3}$$

where $\hat{U}$, $\hat{W}$ and $\hat{u}$, $\hat{w}$ are the directions of radial and axial velocity in the coordinates that are fixed and the coordinates that are moving, respectively.

2.2. Magnetohydrodynamics

The governing equations are comprised of Ampére–Maxwell law, magnetic Gauss law, Faraday's law, and Gauss's law with relation to electric fields [28]:

$$\nabla \times \mathbf{H} = \mathbf{J} + \frac{\partial \mathbf{D}}{\partial t}, \tag{4}$$
$$\nabla \cdot \mathbf{B} = 0, \tag{5}$$
$$\nabla \times \mathbf{E} = -\frac{\partial \mathbf{B}}{\partial t}, \tag{6}$$
$$\nabla \cdot \mathbf{D} = \rho_c. \tag{7}$$

The equations of constitutive, particularly $\mathbf{B}-\mathbf{H}-\mathbf{m}$, $\mathbf{D}-\mathbf{E}-\mathbf{P}$ relations, and OHM's law for fields in motion are next addressed

$$\mathbf{B} = \mu_e \mathbf{H} + \mu_0 \mathbf{m}, \tag{8}$$
$$\mathbf{D} = \varepsilon \mathbf{E} + \mathbf{P}, \tag{9}$$
$$\mathbf{J} = \sigma(\mathbf{E} + \mathbf{V} \times \mathbf{B}). \tag{10}$$

The lorentz force per unit charge

$$\mathbf{F} = \mathbf{E} + \mathbf{J} \times \mathbf{B}, \tag{11}$$

where $\mathbf{V}$, $\mathbf{B}$, $\mathbf{E}$, $\mathbf{J}$, $\mathbf{H}$, $\mathbf{D}$, $\mathbf{P}$, $\mathbf{m}$, ρ_c, μ_e, ε, and σ are respectively the vector of velocity, vector of magnetic field, electric field, vector of current density, the magnetic field density, the electric density vector, the electric polarization, the magnetization, the electric charge density, the magnetic permeability, the electric permeability, and the electrical conductivity.
Since the induced magnetic field is insignificant (thus, $\nabla \times \mathbf{E} = -\frac{\partial \mathbf{B}}{\partial t}$, gives $\mathbf{E} = \mathbf{0}$), when there is no outside electric field. Eqs. (4–11) can be rewritten as follows:

$$\nabla \times \mathbf{H} = \mathbf{J}, \tag{12}$$
$$\nabla \cdot \mathbf{B} = 0, \tag{13}$$
$$\mathbf{B} = \mu_e \mathbf{H}, \tag{14}$$
$$\mathbf{J} = \sigma(\mathbf{V} \times \mathbf{B}), \tag{15}$$

and the Lorentz force as:

$$\mathbf{F} = \mathbf{J} \times \mathbf{B}. \tag{16}$$

In our problem, we take $\mathbf{V} = (\hat{u}, 0, \hat{w})$ and $\mathbf{B} = (\mu_e H_0, 0, 0)$. Eqs. (14) and (15) clearly show that Eq. (16) takes the following form:

$$\mathbf{F} = -\sigma \mu_e^2 H_0^2 \hat{w}\, \hat{e}_z. \tag{17}$$

where H_0 denotes the constant transverse magnetic field and $\hat{e}_z$ denotes the axial unit vector.

2.3. Governing equations

The following are the motion equations and boundary conditions (BCs) utilised in the coordinates that are moving:
continuity equation is

$$\frac{1}{\hat{r}}\frac{\partial(\hat{r}\,\hat{u})}{\partial \hat{r}} + \frac{\partial \hat{w}}{\partial \hat{z}} = 0, \tag{18}$$

Navier–Stokes equations are as follows:

$$\rho\left(\hat{u}\frac{\partial \hat{u}}{\partial \hat{r}}+\hat{w}\,\frac{\partial \hat{u}}{\partial \hat{z}}\right)=-\frac{\partial \hat{P}}{\partial \hat{r}}+\frac{\partial}{\partial \hat{r}}\left(2\hat{\mu}(\hat{r},\hat{z})\frac{\partial \hat{u}}{\partial \hat{r}}\right)+\frac{\partial}{\partial \hat{z}}\left[\hat{\mu}(\hat{r},\hat{z})\left(\frac{\partial \hat{w}}{\partial \hat{r}}+\frac{\partial \hat{u}}{\partial \hat{z}}\right)\right]+\frac{2\hat{\mu}(\hat{r},\hat{z})}{\hat{r}}\left(\frac{\partial \hat{u}}{\partial \hat{r}}-\frac{\hat{u}}{\hat{r}}\right),\quad(19)$$

$$\rho\left(\hat{u}\frac{\partial \hat{w}}{\partial \hat{r}}+\hat{w}\,\frac{\partial \hat{w}}{\partial \hat{z}}\right)=-\frac{\partial \hat{P}}{\partial \hat{z}}+\frac{\partial}{\partial \hat{z}}\left(2\hat{\mu}(\hat{r},\hat{z})\frac{\partial \hat{w}}{\partial \hat{z}}\right)+\frac{1}{\hat{r}}\frac{\partial}{\partial \hat{r}}\left[\hat{r}\,\hat{\mu}(\hat{r},\hat{z})\left(\frac{\partial \hat{w}}{\partial \hat{r}}+\frac{\partial \hat{u}}{\partial \hat{z}}\right)\right]-\sigma\mu_e^2H_0^2\hat{w},\quad(20)$$

and BCs:

$$\frac{\partial \hat{w}}{\partial \hat{r}}=0\ \text{ at }\ \hat{r}=0,\quad(21)$$

$$\hat{w}=-c,\ \hat{u}=-c\frac{d\,\hat{h}}{d\,\hat{z}}\ \text{ at }\ \hat{r}=\hat{h}=\hat{a}+\hat{b}\sin\frac{2\pi}{\lambda}\hat{z},\quad(22)$$

where $\hat{\mu}(\hat{r},\hat{z})$ is the bivariable viscosity function.

2.4. Dimensional Analysis and Approximations

The variables in Eqs. (1–3) and Eqs. (18–22) introducing Reynolds number (Re), wavenumber (δ), and Hartmann number (M) are easy to non-dimensionalize like this:

$$r=\frac{\hat{r}}{\hat{a}},\ R=\frac{\hat{R}}{\hat{a}},\ z=\frac{\hat{z}}{\lambda},\ Z=\frac{\hat{Z}}{\lambda},\ u=\frac{\lambda\,\hat{u}}{\hat{a}\,c},$$
$$U=\frac{\lambda\,\hat{U}}{\hat{a}\,c},\ \mu(r,z)=\frac{\hat{\mu}(\hat{r},\hat{z})}{\mu_0},\ w=\frac{\hat{w}}{c},\ W=\frac{\hat{W}}{c},$$
$$\delta=\frac{\hat{a}}{\lambda}<1,\ Re=\frac{c\hat{a}\rho}{\mu},\ \phi=\frac{\hat{b}}{\hat{a}}<1,\ P=\frac{\hat{P}\,\hat{a}^2}{c\lambda\mu_0},$$
$$t=\frac{c\,\hat{t}}{\lambda},\ M=\mu_eH_0\hat{a}\sqrt{\frac{\sigma}{\mu_0}},\ h=\frac{\hat{h}}{\hat{a}}=1+\phi\sin(2\pi\hat{z}),\quad(23)$$

where ϕ is the occlusion.
After substituting from Eqs. (23), then Eqs. (18–22) are reduced to

$$\frac{1}{r}\frac{\partial(ru)}{\partial r}+\frac{\partial w}{\partial z}=0,\quad(24)$$

$$Re\delta^3\left(u\frac{\partial u}{\partial r}+w\,\frac{\partial u}{\partial z}\right)=-\frac{\partial P}{\partial r}+2\delta^2\frac{\partial}{\partial r}\left(\mu(r,z)\frac{\partial u}{\partial r}\right)+\delta^2\frac{\partial}{\partial z}\left[\mu(r,z)\left(\delta^2\frac{\partial u}{\partial z}+\frac{\partial w}{\partial r}\right)\right]+2\delta^2\frac{\mu(r,z)}{r}\times\left(\frac{\partial u}{\partial r}-\frac{u}{r}\right),\quad(25)$$

$$Re\delta\left(u\frac{\partial w}{\partial r}+w\,\frac{\partial w}{\partial z}\right)=-\frac{\partial P}{\partial z}+\delta^2\frac{\partial}{\partial z}\left(2\mu(r,z)\frac{\partial w}{\partial z}\right)+\frac{1}{r}\frac{\partial}{\partial r}\left[r\mu(r,z)\left(\delta^2\frac{\partial u}{\partial z}+\frac{\partial w}{\partial r}\right)\right]-M^2w,\quad(26)$$

$$\frac{\partial w}{\partial r}=0\ \text{ at }\ r=0,\quad(27)$$

$$w=-1,\ u=-\frac{dh}{dz}\ \text{ at }\ r=h.\quad(28)$$

Assuming that the wavelength is long ($\delta=0$), Eqs. (25) and (26) become

$$\frac{\partial P}{\partial r}=0,\quad(29)$$

$$\frac{\partial P}{\partial z}=\frac{1}{r}\frac{\partial}{\partial r}(r\mu(r,z)\frac{\partial w}{\partial r})-M^2w.\quad(30)$$

In the following formula, Lachiheb [19,20] considers the viscosity of fluid passing through a peristaltic tube and a channel based on radial and axial components:

$$\mu(r,z)=e^{-\frac{\alpha r}{h(z)}}\ or\ \mu(r,z)=1-\frac{\alpha r}{h(z)}\ for\ \alpha<<1\quad(31)$$

where α is the viscosity parameter.

3. Volume Flow Rate

The volume flow rate Q can be computed using the formula

$$Q=2\pi\int_0^{\hat{h}}\hat{R}\hat{W}d\hat{R}\quad(32)$$

where $\hat{h}$ varies with $\hat{t}$ and $\hat{Z}$. Taking Eqs. (2) and (3) and substituting in Eq. (32) after that, the integrated yield

$$Q=\hat{q}+\pi c\,\hat{h}^2,\quad(33)$$

where

$$\hat{q}=\int_0^{\hat{h}}2\pi\hat{w}\hat{r}d\hat{r},\quad(34)$$

is the time-independent volume flow rate in the coordinates that are moving. Here, $\hat{h}$ varies with $\hat{z}$ alone and it is determined by Eq. (22). Using the variables with no dimensions, we get

$$F=\frac{\hat{q}}{2\pi c\hat{a}^2}=\int_0^h rwdr.\quad(35)$$

Over a period $T=\frac{\lambda}{c}$, the time-mean flow at a fixed location $\hat{Z}$ is referred to

$$\hat{Q}=\frac{1}{T}\int_0^T Q\,d\hat{t}.\quad(36)$$

Substituting from Eq. (33) into Eq. (36) after that, the integrated yield

$$\hat{Q}=\hat{q}+\pi c\hat{a}^2(1+\frac{\phi^2}{2}).\quad(37)$$

In terms of determining the time-mean flow with no dimensions Θ as

$$\Theta=\frac{\hat{Q}}{2\pi c\hat{a}^2},\quad(38)$$

Eq. (37) can be rephrased as

$$\Theta=F+\frac{1}{2}(1+\frac{\phi^2}{2}).\quad(39)$$

4. Perturbation Solution

The following is an example of how to solve the current problem analytically using the perturbation approach for small parameters M^2

$$w = w_0 + M^2 w_1 + O(M^4), \quad (40)$$

$$u = u_0 + M^2 u_1 + O(M^4), \quad (41)$$

$$\frac{dP}{dz} = \frac{dP_0}{dz} + M^2 \frac{dP_1}{dz} + O(M^4), \quad (42)$$

$$F = F_0 + M^2 F_1 + O(M^4). \quad (43)$$

Using Eqs. (40–42) as a substitute in Eqs. (24), (29), and (30), we obtain the
zeroth-order system

$$\frac{1}{r}\frac{\partial(ru_0)}{\partial r} + \frac{\partial w_0}{\partial z} = 0, \quad (44)$$

$$\frac{\partial P_0}{\partial r} = 0, \quad (45)$$

$$\frac{\partial P_0}{\partial z} = \frac{1}{r}\frac{\partial}{\partial r}\left(r\,\mu(r,z)\,\frac{\partial w_0}{\partial r}\right), \quad (46)$$

BCs that are dimensionless

$$\frac{\partial w_0}{\partial r} = 0 \text{ at } r = 0, \quad (47)$$

$$w_0 = -1, u_0 = -\frac{dh}{dz} \text{ at } r = h. \quad (48)$$

The first-order system

$$\frac{1}{r}\frac{\partial(ru_1)}{\partial r} + \frac{\partial w_1}{\partial z} = 0, \quad (49)$$

$$\frac{\partial P_1}{\partial r} = 0, \quad (50)$$

$$\frac{\partial P_1}{\partial z} = \frac{1}{r}\frac{\partial}{\partial r}\left(r\,\mu(r,z)\,\frac{\partial w_1}{\partial r}\right) - w_0, \quad (51)$$

BCs that are dimensionless

$$\frac{\partial w_1}{\partial r} = 0 \text{ at } r = 0, \quad (52)$$

$$w_1 = 0, u_1 = 0 \text{ at } r = h. \quad (53)$$

4.1. Solution of the zeroth-order system

Solving Eq. (46) using Eq. (45) with respect to boundary conditions (47) and (48) yields

$$w_0 = \frac{1}{4}\frac{dP_0}{dz}(r^2 - h^2)\left(1 + \frac{2}{3}\alpha\left(\frac{r}{h} - 1\right)\right) - 1. \quad (54)$$

The rate of volume flow F_0 is calculated as follows:

$$F_0 = \int_0^h r w_0 \, dr. \quad (55)$$

Integrating Eq. (55) using Eq. (54) and solving the the outcome for $\frac{dP_0}{dz}$, we obtain

$$\frac{dP_0}{dz} = \frac{-16}{h^4}\left(F_0 + \frac{h^2}{2}\right)\left(1 - \frac{4}{5}\alpha\right). \quad (56)$$

Substituting from Eq. (54) into Eq. (44) utilising the boundary condition (48), the radial velocity u_0 is calculated as follows:

$$u_0 = \frac{rh'}{h^3}\left[4F_0\left(1 - \frac{r^2}{h^2}\right) + \frac{4\alpha}{5}\left(\left(1 - \frac{r}{h}\right)r^2 + 10F_0\left(\frac{2r^2}{5h^2} - \frac{r^3}{3h^3} - \frac{1}{15}\right)\right)\right]. \quad (57)$$

4.2. Solution of first-order system

Eq. (54) is substituted into Eq. (51) and it resolved using Eq. (50), boundary conditions (52) and (53) yield

$$w_1 = \frac{1}{64}(r^4 + 3h^4 - 4r^2h^2)\frac{dP_0}{dz} + \frac{1}{4}\left(\frac{dP_1}{dz} - 1\right)(r^2 - h^2) + \alpha\left[\left(-\frac{h\,r^2}{24}(h + r) + \frac{77h^4}{1200} + \frac{23\,r^5}{1200h}\right)\frac{dP_0}{dz} + \frac{h^2}{6}\left(\frac{r^3}{h^3} - 1\right)\left(\frac{dP_1}{dz} - 1\right)\right]. \quad (58)$$

The rate of volume flow F_1 is calculated as follows:

$$F_1 = \int_0^h r w_1 \, dr. \quad (59)$$

Integrating Eq. (59) using Eq. (58) and solving the outcome for $\frac{dP_1}{dz}$, we obtain

$$\frac{dP_1}{dz} = -\frac{8F_0}{3h^2} - \frac{16F_1}{h^4} - \frac{1}{3} + \frac{8\alpha}{5}\left(\frac{8F_1}{h^4} + \frac{2F_0}{21h^2} + \frac{1}{21}\right). \quad (60)$$

Substituting from Eq. (58) into Eq. (49) using the boundary condition (53), the radial velocity u_1 is calculated as follows:

$$u_1 = h'\left\{\frac{hr}{24}\left(1 - \frac{r^4}{h^4}\right) + \frac{r}{6h^3}\left(r^2F_0\left(1 - \frac{r^2}{h^2}\right) + 24F_1\left(1 - \frac{4r^2}{h^2}\right)\right) + \alpha r\left[\frac{r^4}{30h^3} + \frac{r^3}{45h^2} + \frac{16h}{1575} - \frac{23r^5}{350h^4} + \frac{r^2F_0}{h^3}\left(-\frac{23r^3}{105h^3} + \frac{2r^2}{15h^2} + \frac{2r}{15h} - \frac{1}{21}\right) + \frac{4F_1}{h^3}\left(-\frac{2r^3}{3h^3} + \frac{4r^2}{5h^2} - \frac{2}{15}\right)\right]\right\} \quad (61)$$

We get by substituting from Eqs. (54) and (58) into Eq. (40) using Eq. (42) and disregarding the terms higher than

$O(M^2)$

$$w=\frac{dP}{dz}\left(\frac{1}{4}\left(r^2-h^2\right)+\frac{\alpha}{6}\left(\frac{r^3}{h}-h^2\right)\right)$$
$$+M^2\left[\frac{dP}{dz}\left(\frac{3h^4}{64}+\frac{r^4}{64}-\frac{h^2\,r^2}{16}\right)\right.$$
$$+\alpha\left(\frac{dP}{dz}\left(\frac{77h^4}{1200}+\frac{23r^5}{1200h}-\frac{h\,r^2}{24}(h+r)\right)\right.$$
$$\left.\left.+\frac{1}{6}\left(h^2-\frac{r^3}{h}\right)\right)+\frac{1}{4}\left(h^2-r^2\right)\right]-1. \quad (62)$$

Substituting from Eqs. (57) and (61) into Eq. (41) using Eq. (43) and disregarding the terms larger than $O(M^2)$, we've got

$$u=h'\left\{\frac{r}{h^3}\left(-r^2+\left(1-\frac{r^2}{h^2}\right)4F\right)+\frac{4r\alpha}{5h^3}\left(r^2\left(1-\frac{r}{h}\right)\right.\right.$$
$$\left.+10F\left(\frac{2r^2}{5h^2}-\frac{r^3}{3h^3}-\frac{1}{15}\right)\right)+M^2\left[\frac{rh}{24}\left(1-\frac{r^4}{h^4}\right)\right.$$
$$+\left(1-\frac{r^2}{h^2}\right)\frac{r^3F}{6h^3}+\alpha r\left(-\frac{23r^5}{350h^4}+\frac{r^4}{30h^3}+\frac{r^3}{45h^2}\right.$$
$$\left.\left.\left.+\frac{16h}{1575}+\left(-\frac{23r^3}{105h^3}+\frac{2r^2}{15h^2}+\frac{2r}{15h}-\frac{1}{21}\right)\frac{r^2F}{h^3}\right)\right]\right\} \quad (63)$$

Substituting from Eqs. (56) and (60) into Eq. (42) using Eq. (43) and disregarding the terms larger than $O(M^2)$, we've got

$$\frac{dP}{dz}=\frac{-16}{h^4}\left(F+\frac{h^2}{2}\right)\left(1-\frac{4}{5}\alpha\right)$$
$$-\frac{M^2}{3}\left[1+\frac{8F}{h^2}-\frac{8\alpha}{35}\left(1+\frac{2F}{h^2}\right)\right]. \quad (64)$$

The pressure rising ΔP_λ and drag (friction) forces F_λ can be expressed by

$$\Delta P_\lambda=\int_0^1\left(\frac{dP}{dz}\right)dz, \quad (65)$$

$$F_\lambda=\int_0^1 h^2\left(-\frac{dP}{dz}\right)dz. \quad (66)$$

Using the formula of Eq. (64), Eqs. (65) and (66) become

$$\Delta P_\lambda=2\left(1-\frac{4}{5}\alpha\right)\left(\frac{\left(2-4\Theta+\phi^2\right)\left(2+3\phi^2\right)}{\left(1-\phi^2\right)^{7/2}}\right.$$
$$\left.-\frac{4}{\left(1-\phi^2\right)^{3/2}}\right)+\frac{M^2}{105}\left[4\alpha\left(2-\frac{2-4\Theta+\phi^2}{\left(1-\phi^2\right)^{3/2}}\right)\right.$$
$$\left.-35\left(1-\frac{2\left(2-4\Theta+\phi^2\right)}{\left(1-\phi^2\right)^{3/2}}\right)\right], \quad (67)$$

$$F_\lambda=4\left(1-\frac{4}{5}\alpha\right)\left(2+\frac{4\Theta-2-\phi^2}{\left(1-\phi^2\right)^{3/2}}\right)$$
$$-M^2\left(1+\frac{\phi^2}{2}+\frac{8}{3}\Theta\left(1-\frac{2\alpha}{35}\right)\right). \quad (68)$$

Furthermore, we obtain the solutions to the equations given in Eqs. (44–53) in the following ways as $\mu=\mu(r)$:

$$w=\frac{dP}{dz}\left(\frac{1}{4}(r^2-h^2)+\frac{\alpha}{6}(r^3-h^3)\right)$$
$$+M^2\left[\frac{dP}{dz}\left(\frac{3h^4}{64}+\frac{r^4}{64}-\frac{h^2\,r^2}{16}\right)+\frac{1}{4}(h^2-r^2)\right.$$
$$+\frac{\alpha}{24}\left(\frac{dP}{dz}\left(\frac{1}{50}\left(23r^5+77h^4\right)-h\,r^2(h+r)\right)\right.$$
$$\left.\left.+4(h^3-r^3)\right)\right]-1, \quad (69)$$

$$u=h'\left\{\frac{r}{h^3}\left(4F\left(1-\frac{r^2}{h^2}\right)-r^2\right)\right.$$
$$+\frac{2}{5}\alpha r\left(\frac{1}{3}+\frac{2F}{3h^2}\left(-\frac{8r^3}{h^3}+\frac{9r^2}{h^2}-1\right)\right)$$
$$+M^2\left[\frac{rh}{24}\left(1-\frac{r^4}{h^4}\right)+\frac{r^3F}{6h^3}\left(1-\frac{r^2}{h^2}\right)\right.$$
$$+\frac{\alpha r}{84}\left(r^2+\frac{32h^2}{25}-\frac{92r^5}{25h^3}+\frac{7r^4}{5h^2}\right.$$
$$\left.\left.\left.+Fr\left(\frac{16}{1575}-\frac{92r^5}{525h^5}+\frac{r^4}{10h^4}+\frac{4r^3}{45h^3}-\frac{r^2}{42h^2}\right)\right)\right]\right\}, \quad (70)$$

$$\frac{dP}{dz}=\frac{-16}{h^4}\left(F+\frac{h^2}{2}\right)\left(1-\frac{4}{5}\alpha h\right)$$
$$-\frac{M^2}{3}\left(1+8F-\frac{8h\alpha}{35}\left(1+\frac{2F}{h^2}\right)\right), \quad (71)$$

$$\Delta P_\lambda=-\frac{8}{\left(1-\phi^2\right)^{3/2}}+\frac{2\left(2-4\Theta+\phi^2\right)\left(2+3\phi^2\right)}{\left(1-\phi^2\right)^{7/2}}$$
$$+\frac{8\alpha}{5}\left(-\frac{\left(2-4\Theta+\phi^2\right)\left(2+\phi^2\right)}{\left(1-\phi^2\right)^{5/2}}+\frac{4}{\left(1-\phi^2\right)^{1/2}}\right)$$
$$+\frac{M^2}{105}\left[-35\left(1-\frac{2\left(2-4\Theta+\phi^2\right)}{\left(1-\phi^2\right)^{3/2}}\right)\right.$$
$$\left.+4\alpha\left(2-\frac{2-4\Theta+\phi^2}{5\left(1-\phi^2\right)^{1/2}}\right)\right], \quad (72)$$

and

$$F_\lambda=4\left(2-\frac{2-4\Theta+\phi^2}{\left(1-\phi^2\right)^{3/2}}\right)+\frac{16\alpha}{5}\left(\frac{2-4\Theta+\phi^2}{\left(1-\phi^2\right)^{1/2}}-2\right)$$
$$+M^2\left(1+\frac{\phi^2}{2}-\frac{8}{3}\Theta+\frac{8\alpha}{105}\left(2\Theta+\phi^2\right)\right). \quad (73)$$

5. Separated Flow (Trapping at the Boundary)

Setting the vorticity on the boundary equal to zero is a common condition used in boundary layer theory to anticipate separation

$$\xi = \frac{\partial u}{\partial z} - \frac{\partial w}{\partial r} = 0 \qquad \text{on} \qquad r = h. \qquad (74)$$

we get, by substituting from Eqs. (62) and (63) into Eq. (74)

$$h^3 h'' - 4(2F + h^{2)} - \left(8F + 3h^2\right) h'^2 - \frac{4\alpha}{5}\left(2F + h^2\right)\left(1 + h'^2\right) - \frac{h^2 M^2}{6}\left(1 + \frac{27h^2\alpha}{35}\right)\left(2F + h^2\right)\left(1 + h'^2\right) = 0. \qquad (75)$$

Substituting Eq. (23) into Eq. (75), we obtain

$$0 = 4\left[\left(1 + \pi^2\phi\left(2\phi + \phi\cos(4\pi z) + \sin(2\pi z)\right)\right)(1 + \phi\sin(2\pi z))^2 + 2F\left(2\pi^2\phi^2(1 + \cos(4\pi z)) + 1\right)\right] + \frac{4\alpha}{5}\left[\left(1 + 2\pi^2\phi^2(1 + \cos(4\pi z))\right)(\phi\sin(2\pi z) + 1)^2 + 2F\left(1 + 2\pi^2\phi^2(1 + \cos(4\pi z))\right)\right] + \frac{M^2}{420}(1 + \phi\sin(2\pi z))^2(35 + 27\alpha)\left(1 + 2\pi^2\phi^2(1 + \cos(4\pi z))\right)\left[\left(\phi^2(1 - \cos(4\pi z)) + 2(1 + 2F + 2\phi\sin(2\pi z))\right)\right]. \qquad (76)$$

To obtain flow points z_s that are separate at the wall surface for $\mu = \mu(r,z)$, we solve Eq. (76) numerically. In addition, we obtain separated flow points z_s for $\mu = \mu(r)$ by solving numerically the following equation:

$$0 = 4\left[\left(1 + \pi^2\phi\left(2\phi + \phi\cos(4\pi z) + \sin(2\pi z)\right)\right)(1 + \phi\sin(2\pi z))^2 + 2F\left(2\pi^2\phi^2(1 + \cos(4\pi z)) + 1\right)\right] + \frac{4\alpha}{5}\left[\left(1 + 4\pi^2\phi^2\cos^2(4\pi z)\right)(1 + \phi\sin(2\pi z))^2 + 2F\left((1 + \phi\sin(2\pi z))\left(1 + 2\pi^2\phi^2(1 + \cos(4\pi z))\right)\right)\right] \frac{M^2}{420}\left[35 + 27\alpha(1 + \phi\sin(2\pi z))\right]\left[1 + 2\pi^2(1 + \cos(4\pi z))\phi^2\right](\phi\sin(2\pi z) + 1)^2\left[\phi^2(1 - \cos(4\pi z)) + 2(1 + 2\phi\sin(2\pi z) + 2F)\right] \qquad (77)$$

6. Numerical Results and Discussion

We derive analytical solutions to the governing equations for peristaltic flow of a Newtonian fluid with bivariation viscosity in the presence of a magnetic field using a succession of regular perturbations when it comes to the Hartmann number M. A digital computer was used to perform computations for different values of the parameter of viscosity α, occlusion ϕ, Hartmannnumber M, and volume flow rate Θ to analyze the behaviour of solutions. Pressure rise and volume flow rate of a fluid whose viscosity can be either bivariation or a function of a radial component relationships given by Eqs. (67) and (72), respectively, are drawn in Figs. 2–4. Moreover, the relations between drag (friction) forces and volume flow rate of these types of fluids provided by Eqs. (68) and (73), respectively, are drawn in Figs. 5–7. To discuss the results quantitatively, these are the parameter values that we used: $\hat{a} = 1.25cm$, $c = 2\text{cm/min}$ and $\lambda = 8.01cm$, as given in references [6, 7]. The viscosity parameter α for these types of fluids takes values 0 and 0.1, as reported in the study by Srivastava et al. [7]. The small Hartmann number M takes values $0, 0.3$, and 0.5, as given in reference [23].

Figs. 2–4 show that as the volume flow rate increases, the magnitude of the pressure rise decreases in the region of peristaltic pumping, where $\Theta > 0$ and $\Delta P_\lambda > 0$, but it rises as the volume flow rate rises in the region of augmented pumping, where $\Theta > 0$ and $\Delta P_\lambda < 0$, for a fluid with bivariation viscosity $\mu(r,z)$ and a fluid with radial viscosity $\mu(r)$. This result indicates that peristaltic pumping happens when the velocity field of the flow increases in a contraction area., whereas augmented pumping happens in a relaxation region in which the velocity field of the flow decreases. Moreover, the pressure rise of a fluid with bivariation viscosity is smaller than that of a fluid with radial viscosity. This phenomenon occurs because the viscosity of a fluid with bivariation viscosity is smaller than the viscosity of a fluid with radial viscosity for small viscosity parameter α. Furthermore, the pressure rise is approximately independent of small Hartmann number M for various values of the volume flow rate of these fluids as shown in Fig. 3. In addition, peristaltic pumping happens at $0 < \Theta \leq 0.08$ for small occlusion $(\phi = 0.2)$ and at $0 < \Theta \leq 0.46$ for high occlusion $(\phi = 0.6)$; otherwise, augmented pumping happens for these fluids as illustrated in Fig. 4.

Figs. 5–7 demonstrate that the magnitude of drag (friction) forces decreases as the volume flow rate rises in the region of peristaltic pumping, where $\Theta > 0$ and $F_\lambda < 0$, but it rises as the volume flow rate rises in the reflux (backward flow) region, where $\Theta > 0$ and $F_\lambda > 0$, for a fluid with bivariation viscosity $\mu(r,z)$ and a fluid with radial viscosity $\mu(r)$. Moreover, the friction force of a fluid with bivariation viscosity is smaller than that of a fluid with radial viscosity. Furthermore, the friction force is approximately independent of small Hartmann number M for various values of the volume flow rate of these fluids, as shown in Fig. 6. Peristaltic pumping happens approximately at $0 < \Theta \leq 0.05$ for small occlusion $(\phi = 0.2)$ and at $0 < \Theta \leq 0.34$ for high occlusion $(\phi = 0.6)$; otherwise, backward flow happens for these fluids, as illustrated in Fig. 7.

Trapping phenomenon was studied by several investigators. A bolus (a volume of fluid restricted in the frame of the wave by closed streamlines) is conveyed at the speed of the wave, causing trapping at the centerline. As previously explained by Siddiqui and Schwarz [29], the trapping limits are calculated by computing the proportion of the $\Theta_{\min}$ (minimum volume flow rate) and $\Theta_{\max}$ (maximum volume flow rate) in relation to occlusion ϕ. Eq. (62) gives us the minimum volume flow rate $\Theta_{\min}$ when $w = 0$, $r = 0$ and $h = 1 + \phi$ and solving the outcome for Θ. Substituting $\Delta P_{\lambda} = 0$ in Eq. (67) and solving the outcome for Θ, we achieve then $\Theta_{\max}$. Physically, $\Theta_{\min}$ and $\Theta_{\max}$ must be real and address inequity $0 \leq \Theta_{\min} \leq \Theta_{\max}$. Therefore, trapping happens such that $0 \leq \frac{\Theta_{\min}}{\Theta_{\max}} \leq 1$ for all possible M, ϕ, and α values as shown in Figs. 8 and 9, which are graphs of $\frac{\Theta_{\min}}{\Theta_{\max}}$ against the occlusion ϕ for the cases $\{\alpha = 0.1;\ M = 0, 0.3,$ and $0.5\}$ and $\{M = 0.3;\ \alpha = 0, 0.1\}$, respectively. The graphs show that the trapping limits increase with increasing small Hartmann number M and the small viscosity parameter α. Moreover, the trapping limits are smaller for bivariation viscosity than for viscosity as a function of a radial component. Furthermore, Shapiro et al. [2] found trapping limits that match our results at $M = 0$ and $\alpha = 0$.

We discuss the separated flow phenomena (trapping on the boundary) by way of Figs. 10–12, which show the relationship between the axial component z_s of separation flow points and occlusion ϕ. The graphs show at certain values of volume flow rate Θ, Hartmann number M, amplitude ratio ϕ, and viscosity parameter α that z_s bifurcates into two branches. One of them (upper branch) approaches the contraction region's exit, on the other hand (lower branch) approaches the contraction region's inlet. Fig. 10 shows that the trapping region happens in the contraction region for various volume flow rate values but happens in the relaxation region only at $\{M = 0.3,$ $\alpha = 0.1$, and $\Theta = 0.2\}$. In addition, Fig. 10 clearly shows fixed points (critical amplitude ratios) that interchange their stability with other fixed points as the parameter Θ changes. Thus, bifurcations of flow occur through a uniform tube with peristalsis. Figs. 10–12 demonstrate that the flow's non-separation points happen approximately at $\{\{0 < \phi < 0.04,\ \Theta = 0.2\}$, $\{0 < \phi < 0.08,\ \Theta = 0.4\}$, $\{0 < \phi < 0.16,\ \Theta = 0.6\}$, $M = 0.3$, $\alpha = 0.1\}$, $\{0 < \phi < 0.12$, $\Theta = 0.5$, $\alpha = 0.1$, for different values of $M\}$, and $\{0 < \phi < 0.11,\ \Theta = 0.5,$ $\alpha = 0$, and $M = 0.3\}$. The non-separation region increases with an increasing volume flow rate Θ. In addition, as the volume flow rate Θ increases, z_s increases in the contraction region's inlet and decreases as Θ increases in the contraction region's exit. Moreover, Fig. 11 shows that z_s is approximately unaffected by the small Hartmann number M at $\{\alpha = 0.1,\ \Theta = 0.5\}$. Furthermore, z_s is approximately unaffected by the small viscosity parameter α at $\{M = 0.3,\ \Theta = 0.5\}$, as shown in Fig. 12. As shown in Figs. 11 and 12, the axial component of flow points that are separated for a fluid whose viscosity can be either bivariation or a function of a radial component is approximately the same.

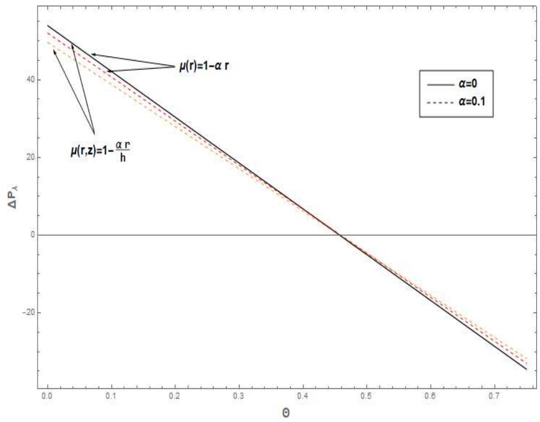

Fig. 2: The pressure rise ΔP_{λ} against the volume flow rate Θ at $M = 0.3$ and $\phi = 0.6$

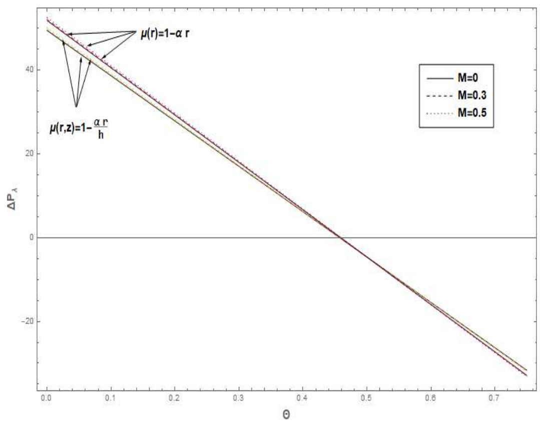

Fig. 3: The pressure rise ΔP_{λ} against the volume flow rate Θ at $\alpha = 0.1$ and $\phi = 0.6$

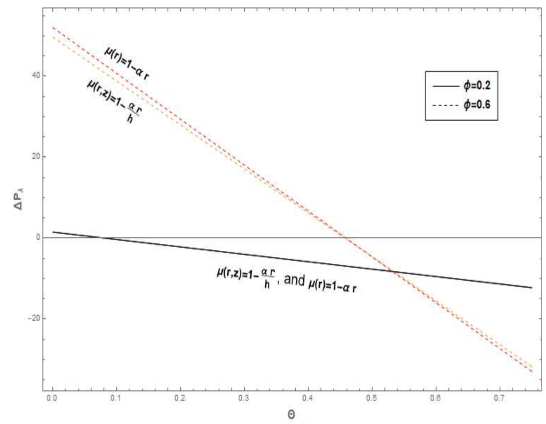

Fig. 4: The pressure rise ΔP_{λ} against the volume flow rate Θ at $M = 0.3$ and $\alpha = 0.1$

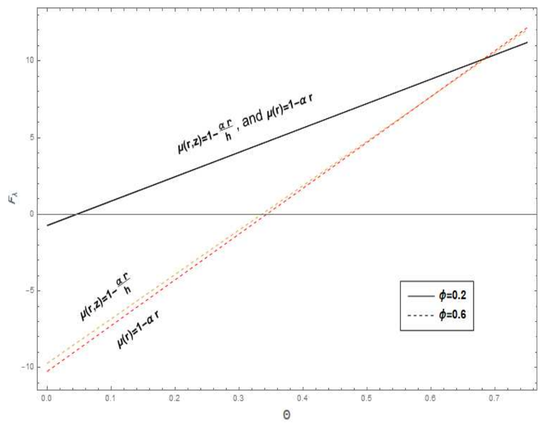

Fig. 7: The friction force F_{λ} versus the volume flow rate Θ at $M = 0.3$ and $\alpha = 0.1$

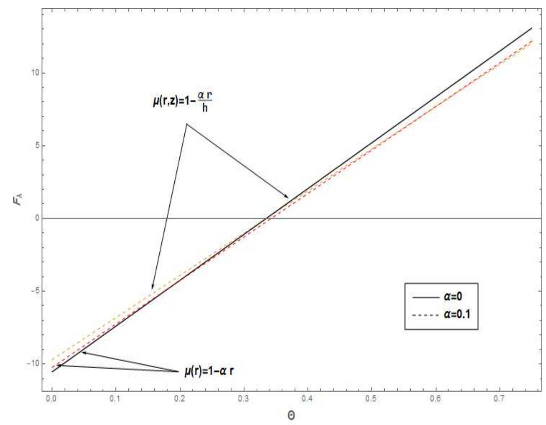

Fig. 5: The friction force F_{λ} versus the volume flow rate Θ at $M = 0.3$ and $\phi = 0.6$

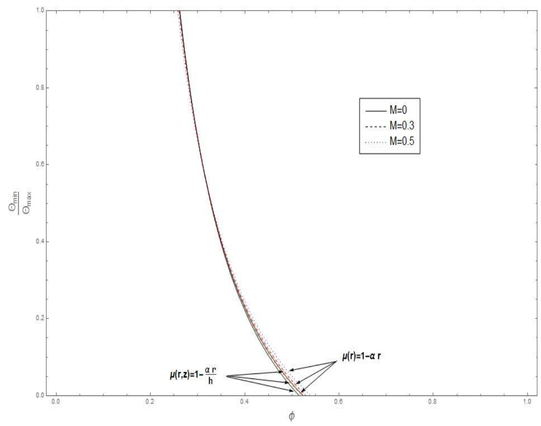

Fig. 8: $\frac{\Theta_{\min}}{\Theta_{\max}}$ versus amplitude ratio ϕ at $\alpha = 0.1$

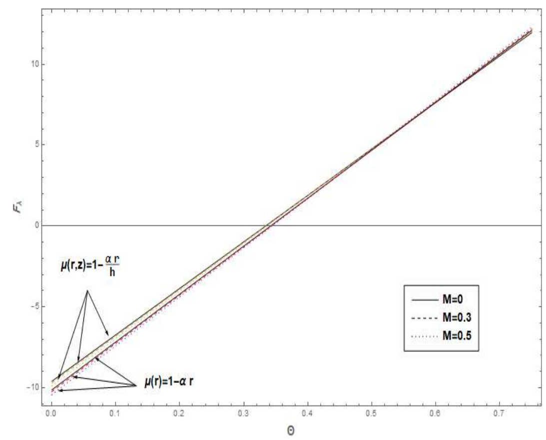

Fig. 6: The friction force F_{λ} versus the volume flow rate Θ at $\alpha = 0.1$ and $\phi = 0.6$

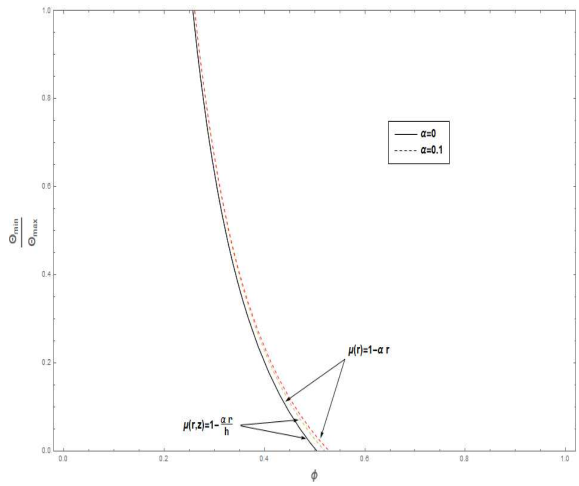

Fig. 9: $\frac{\Theta_{\min}}{\Theta_{\max}}$ versus amplitude ratio ϕ at $M = 0.3$

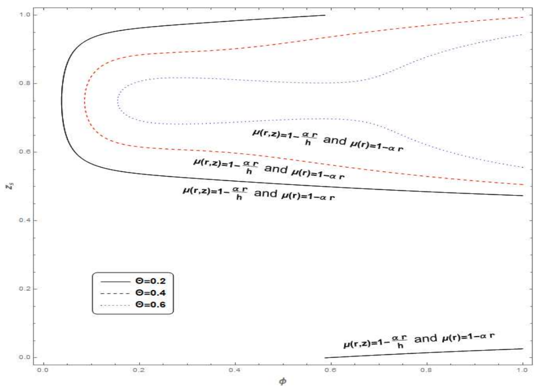

Fig. 10: The axial component of flow separation points z_s versus amplitude ratio ϕ at $\alpha = 0.1$ and $M = 0.3$

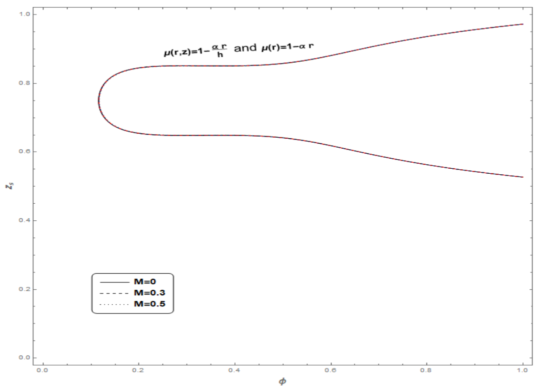

Fig. 11: The axial component of flow separation points z_s versus amplitude ratio ϕ at $\alpha = 0.1$ and $\Theta = 0.5$

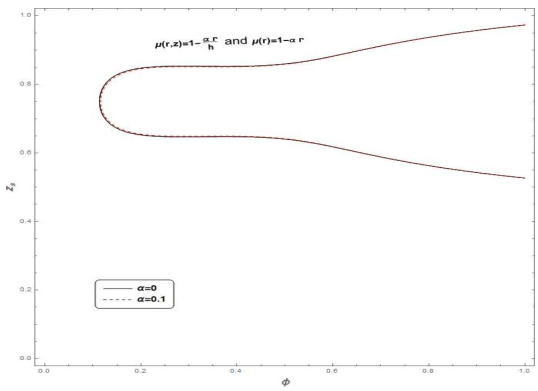

Fig. 12: The axial component of flow separation points z_s versus amplitude ratio ϕ at $M = 0.3$ and $\Theta = 0.5$

7. Conclusion

As a result of previous analyses, we conclude that the flow field of a fluid with bivariation viscosity through a peristaltic tube in presence of a magnetic field is remarkable. More exactly:

• The small viscosity parameter (α) of a fluid whose viscosity is bivariation and a fluid whose viscosity is a function of a radial component affects the pressure rise and the drag (friction) forces. However, a small Hartmann number (M) affects neither the pressure rise nor the drag (friction) forces for a variety of flow rate values.

• The small occlusion $(\phi = 0.2)$ of the peristaltic wave affects neither the pressure rise nor the drag (friction) forces of a fluid whose viscosity can be either a bivariation or a function of a radial component. However, high occlusion $(\phi = 0.6)$ affects the pressure rise and the drag (friction) forces of these types of fluids for a variety of flow rate values.

• The small Hartmann number and small viscosity parameter of the mentioned fluids affect the centerline's trapping limit of the peristaltic tube.

• The small Hartmann number and small viscosity parameter of the mentioned fluids do not affect the flow points that are separated (trapping) at the wall surface, but volume flow rate affects these points for a variety of amplitude ratio values.

Conflicts of Interests

The authors declare that they have no conflicts of interests

References

[1] T.W. Latham. Fluid motions in a peristaltic pump. M S Thesis, M I T. (1966).
[2] A.H. Shapiro, M.Y. Jaffrin, S.L. Weinberg, Peristaltic pumping with long wavelengths at low Reynolds number, J Fluid Mech. 37 (1969), no. 4, 799–825.
[3] M. Mishra, A. R. Rao, Peristaltic transport of a Newtonian fluid in an asymmetric channel, Z. angew. Math. Phys. 54 (2003), no. 4, 532-550.
[4] J.C. Burns, T. Parkes, Peristaltic motion, J. Fluid Mech. 29 (1967) 731-743.
[5] T.F. Zien, S. Ostrach, A longwave approximation to peristaltic motion, J. Biomech. 3 (1970), no. 4, 63-75.
[6] J.B. Shukla, R.S. Parihar, B.R.P. Rao, S.P. Gupta, Effects of peripheral layer viscosity on peristaltic transport of a bio-fluid, J. Fluid Mech. 97 (1980) 225-237.
[7] L.M. Srivastava, V.P. Srivastava, S.N. Sinha, Peristaltic transport of a physiological fluid. Part-I. Flow in non-uniform geometry, Biorheology. 20 (1983) 153-166.
[8] L.M. Srivastava, V.P. Srivastava, S.N. Sinha, Peristaltic transport of a physiological fluid. Part-II. Flow in uniform geometry, Biorheology. 20 (1983) 167-178.
[9] A.E.M. El Misery, A.E.H. Abd El Naby, A.H. El Nagar, Effects of a fluid with variable viscosity and an endoscope on peristaltic motion, J. Phys. Soc. Jpn. 72 (2003) 89-93.
[10] A.E.H. Abd El Naby, A.E.M. El Misiery, I.I. El Shamy, Hydromagnetic flow of fluid with variable viscosity in a uniform tube with peristalsis, J. Phys. A: Math. Gen. 36 (2003) 8535-8547.
[11] A.E.H. Abd El Naby, A.E.M. El Misery, I.I. El Shamy, Effects of an endoscope and fluid with variable viscosity on

peristaltic motion, Appl. Math. Comput. 158 (2004) 497-511.
[12] E.F. Elshehawey, Z.M. Gharsseldien, Peristaltic transport of three-layered flow with variable viscosity, Appl. Math. Comput. 153 (2004) 417-432.
[13] N. T. Eldabe, E. M. Elghazy, A. Ebaid, Closed form solution to a second order boundary value problem and its application in fluid mechanics, Phys. Lett. A. 363 (2007) 257-259.
[14] A. Sinha, J.C. Misra, MHD flow of blood through a dually stenosed artery: effects of viscosity variation, variable hematocrit and velocity-slip, Can. J. Chem. Eng. 92 (2014) 23-31.
[15] G. C. Shit, M. Roy, A. Sinha, Mathematical modelling of blood flow through a tapered overlapping stenosed artery with variable viscosity, Appl. Bionics Biomech. 11 (2014) 185-195.
[16] S. Akram, E. H. Aly, F. Afzal, S. Nadeem, Effect of the Variable Viscosity on the Peristaltic Flow of Newtonian Fluid Coated withMagnetic Field: Application of Adomian Decomposition Method for Endoscope, Coatings. 9 (2019) 524-544.
[17] S. Gupta, M. Gupta, a study of axial viscosity variation in an artery with mild stenosis: bingham-plastic fluid model, Int. J. of Appl. Math and Mech. 10 (2014) 38-46.
[18] A. Singh, P. Singh, effect of axial viscosity variation through an atherosclerotic artery: a non-newtonian fluid model, Int. J. Curr. Eng. Sci. Res (IJCESR), 3 (2016) 69-75.
[19] M. Lachiheb, Effect of coupled radial and axial variability of viscosity on the peristaltic transport of Newtonian fluid, Appl. Math. Comput. 244 (2014) 761-771.
[20] M. Lachiheb. A bivariate viscosity function on the peristaltic motion in an asymmetric channel, ARPN J. Eng. Appl Sci. 13 (2018) 2038-2050.
[21] A.E.H. Abd El Naby, A.E.M. El Misery, M.F. Abd El Kareem, Separation in the flow through peristaltic motion of a carreau fluid in uniform tube, Physica A. 343 (2004) 1-14.
[22] A.E.H. Abd El Naby, A.E.M. El Misery, M.F. Abd El Kareem, Effects of a magnetic field on trapping through peristaltic motion for generalized Newtonian fluid in channel, Physica A. 367 (2006) 79-92.
[23] A.E.H. Abd El Naby, A.E.M. El Misery, I. El Shamy, Hydromagnetic flow of generalized Newtonian fluid through a uniform tube with peristalsis, Appl. Math. Comput. 173 (2006) 856-871.
[24] A.E.H. Abd El Naby, A.E.M. El Misery, M.F. Abd El Kareem, hydro-magnetic flow effects in uniform tube through peristaltic motion for generalized newtonian fluid on trapping, Multidiscip. Model. Mat. Str. 3 (2007) 491-504.
[25] A.E.H. Abd El Naby, M.F. Abd El Kareem, The Flow Separation through Peristaltic Motion for Power-law Fluid in Uniform Tube, Appl. Math. Sci. 1 (2007) 1249-1263.
[26] N. T. Eldabe, O. M. Abo-Seida, A. A. S. Abo-Seliem, A. A. ElShekhipy, N. Hegazy, Peristaltic Transport of Magnetohydrodynamic Carreau Nanofluid with Heat and Mass Transfer inside Asymmetric Channel, Am. J. Comput. Math. 7 (2017) 1-20.
[27] N. T. Eldabe, A. A. Zaghrout, S. F. Ramadan, H. A. Azzam, Simultaneous effects of radiation, magnetic field on peristaltic flow of Carreau nanofluid submerged in gyrotactic microorganisms with heat and mass transfer, Heat Transfer. 50 (2020) 1-20.
[28] Linz, Marz, "Introduction to Magnetohydrodynamics," Johannes Kepler Universitat, (2016).
[29] A. M. Siddiqui, W. H. Schwarz, Peristaltic motion of a third-order fluid in a planar channel, Rheol. Acta. 32 (1993) 47-56.